Near-infrared-to-near-infrared down-shifting and upconversion luminescence of KY_3F_{10} with single dopant of Nd^{3+} ion

Huihong Lin, Ting Yu, Ming-Kiu Tsang, Gongxun Bai, Qinyuan Zhang [iD], and Jianhua Hao

View Online   Export Citation   CrossMark

ARTICLES YOU MAY BE INTERESTED IN

Near-infrared-to-near-infrared down-shifting and upconversion luminescence of KY_3F_{10} with single dopant of Nd^{3+} ion

Huihong Lin,[1,2] Ting Yu,[2] Ming-Kiu Tsang,[1,3] Gongxun Bai,[1,3] Qinyuan Zhang,[2] and Jianhua Hao[1,3,a)]

[1]*Department of Applied Physics, The Hong Kong Polytechnic University, Hong Kong, People's Republic of China*
[2]*State Key Laboratory of Luminescence Materials and Devices and Institute of Optical Communication Materials, South China University of Technology, Guangzhou 510641, People's Republic of China*
[3]*The Hong Kong Polytechnic University Shenzhen Research Institute, Shenzhen 518057, People's Republic of China*

We have studied the structural and near-infrared (NIR) luminescent properties of KY_3F_{10} phosphors, singly doped with Nd^{3+} serving as both sensitizer and activator. With a single laser diode at the wavelength of 808 nm as a pump source, simultaneous NIR-to-NIR upconversion (UC) and down-shifting (DS) emissions are effectively achieved, due to the specific energy levels of Nd^{3+} dopant and the low phonon energy of the host. The luminescence mechanism related to energy transfer is discussed. The luminescence can be modulated through controlling the population of $Nd^{3+}:^4F_{3/2}$ state in our experiment. Interestingly, both UC and DS emissions of the material fall within the dual biological window, suggesting that the prepared phosphors have potential applications in the bioimaging field. © 2016 AIP Publishing LLC. [http://dx.doi.org/10.1063/1.4940747]

Upconversion (UC) is a process in which the sequential absorption of two or more photons leads to the emission of light at shorter wavelength than the excitation wavelength. It is an anti-Stokes type emission. A number of UC examples are based on the conversion of near-infrared (NIR) light to visible (VIS) light.[1–3] The classic NIR-to-VIS UC phenomenon occurs in most trivalent lanthanide ions doped materials, such as Er^{3+}, Tm^{3+}, Pr^{3+}, and Ho^{3+}.[4–7] At present, there is a great interest in luminescent materials for efficient frequency conversion from NIR to NIR radiation, mainly due to its promise for the use in the bioimaging field. NIR-to-NIR phosphors are greatly beneficial to minimizing autofluorescence and achieving the deeper penetration of the biological system, since both the excitation and emission wavelengths fall within the biological transparency window [650–950 nm (first NIR window, NIR I) and 1000–1350 nm (second NIR window, NIR II)].[8–10] Our previous work indicates that NIR-to-NIR UC can be realized in Yb^{3+}/Tm^{3+} doped GdF_3 under 980 nm excitation.[11] However, it is known that 980 nm light used for pumping Yb^{3+}-sensitized UC nanoparticles (UCNPs) may be absorbed by the water component in a biological tissue,[12] limiting the penetration depth and causing severe overheating effects. In order to avoid these shortcomings, utilization of 808 nm light as an excitation source is a more favorable choice, which has become a trend in the biolabel research.

Nd^{3+} ion is considered as a good candidate for improving the pumping efficiency of 808-nm laser diode (LD), due to its large absorption cross-section around 800 nm.[13] For example, the absorption cross-section of Nd^{3+} (1.2×10^{-19} cm^2 at 808 nm) is ten times larger than Yb^{3+} (1.2×10^{-20} cm^2 at 980 nm) in YAG crystal.[14,15] The electron configuration of Nd^{3+} is $[Xe]4f^3$. As the energy levels derived from the $4f^3$ configuration are well shielded from the crystal field, there is only slight variation in the laser wavelengths from one host crystal to another. The energy level structure of Nd^{3+} shows a multitude of levels, and many of them are emissive.[16,17] Unfortunately, Nd^{3+} is usually employed as a sensitizer only rather than an activator in many UC materials where the absorbed energy by Nd^{3+} is transferred to the other ions (e.g., Yb^{3+}, Tm^{3+}, and Er^{3+}) as activators.

In addition, NIR-to-NIR down-shifting (DS) emission provides an alternative to UC because of its higher quantum yield.[18] Therefore, the ideal fluorescent probe would consist of a dual mode in a single compound in which UC and DS luminescence should be complementary to each other. It is seldom to report on the simultaneous realization of NIR-to-NIR UC and DS luminescence in a single ion doped specific system under single wavelength excitation which can greatly facilitate and simplify the phosphor's formula and measurement. Nd^{3+} single doped UC materials can be found in $BaCl_2$ single crystal or $BaCl_2$ glass ceramics under ∼800 nm laser diode excitation. It showed an intense visible UC emission, due to a quite low phonon energy of $BaCl_2$.[19,20] In this work, we choose KY_3F_{10} as a host with relatively low phonon energy (∼400 cm^{-1}), benefiting for reducing nonradiative relaxation.[21] Importantly, NIR-to-NIR UC and DS emissions are simultaneously observed in $KY_3F_{10}:Nd^{3+}$ phosphors under the single NIR light (808 nm) excitation. The energy transfer mechanisms of NIR-to-NIR UC and DS are illustrated to explain the observation.

The $KY_{2.97}Nd_{0.03}F_{10}$ samples were synthesized using anhydrous KF, YF_3, and NdF_3 powders with the chemical formula of $1.05KF$-$2.97YF_3$–$0.03NdF_3$ by a conventional solid-state reaction technique. An excessive mass of KF was added by considering volatile KF. The mixtures were

---

a)Author to whom correspondence should be addressed. Electronic mail: jh.hao@polyu.edu.hk
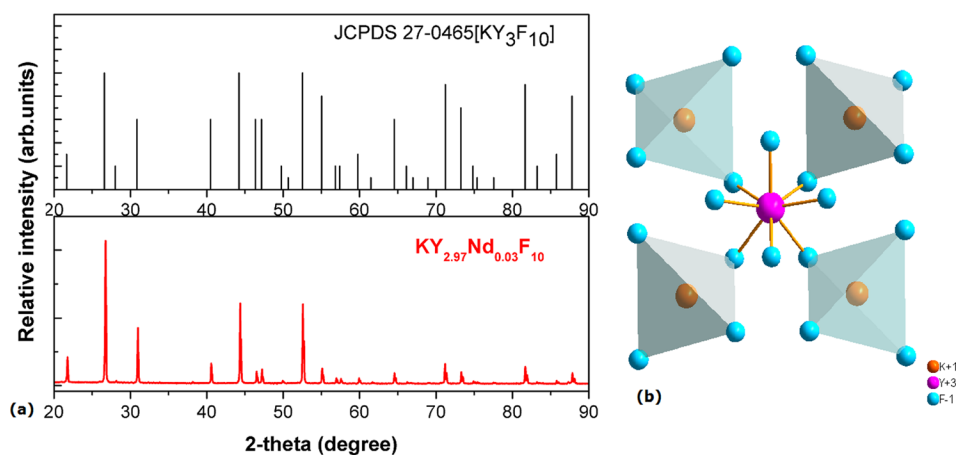
FIG. 1. (a) XRD patterns of the sample $KY_{2.97}Nd_{0.03}F_{10}$. (lower). The KY_3F_{10} PDF standard card is shown for comparison (upper). (b) Schematic diagram of structure and coordination environment of the K^+ and Y^{3+} cations.

grounded homogeneously and then preheated at 250 °C in a pure nitrogen atmosphere for 2 h and finally sintered at 750 °C for 10 h. The phase identification of the obtained products were analyzed by X-ray powder diffractometer (XRD). The photoluminescence (PL) spectra were characterized using a spectrofluorimeter equipped with various excitation sources. All measurements were carried out at room temperature.

Fig. 1(a) shows the XRD patterns of the KY_3F_{10} standard card (JCPDS 27-0465) and the sample $KY_{3-x}Nd_xF_{10}$ ($x = 0.03$). It can be observed that the as-prepared $KY_{2.97}Nd_{0.03}F_{10}$ is in a good agreement with standard KY_3F_{10} compound, suggesting that the substitution of Y^{3+} by Nd^{3+} does not significantly influence the crystal structure. The crystal structure of KY_3F_{10} was reported to possess a cubic compound with space group O_h^5 ($Fm\bar{3}m$).[22] Trivalent rare-earth ions of Nd^{3+} dopant here substitute for the Y^{3+} ion and thus reside on a site of C_{4v} point group symmetry. The K is coordinated tetrahedrally by four inner fluorine atoms at distances of approximately 270 pm. The schematic diagram of the KY_3F_{10} structure and coordination environment of the K^+ and Y^{3+} cations are displayed in Fig. 1(b). The KY_3F_{10} host is very stable and there is no structural phase transition observed in the temperature range of 298–800 K.[23]

Fig. 2 shows the measured UC emission spectra of $KY_{2.97}Nd_{0.03}F_{10}$ sample upon 808 nm LD excitation with different power. With the increase in irradiated power, the PL spectra show three main bands centered at around 685, 737, and 744 nm along with minor emission band at around 587 nm. The inset (a) of Fig. 2 shows the pump power dependence of the overall UC emissions at 685, 737, and 744 nm. An approximate quadratic dependence (slope = 2.27) implies that a two-photon UC process dominates the observed UC PL.

It is noticeable that the three main bands were seldom observed in other Nd-doped materials.[24] Hence, the energy level diagram of Nd^{3+} was analyzed. As shown in Fig. 3, the observed emission bands in UC PL spectra should originate from the $^4G_{7/2}$ and $^2G_{9/2}$ levels. Specifically, the emissions at 685 nm, 737 nm, and 744 nm are attributed to the energy transitions of $^4G_{7/2} \rightarrow {}^4I_{13/2}$, $^2G_{9/2} \rightarrow {}^4I_{15/2}$, and $^4G_{11/2} \rightarrow {}^4I_{15/2}$, respectively. Additionally, the emission intensity at 587 nm corresponded to $^4G_{7/2} \rightarrow {}^4I_{11/2}$ transition is too weak to be counted in the following fitting calculation; the ratio of $I_{587}/(I_{685} + I_{737})$ versus 808 nm laser excitation power is shown in the inset (b) of Fig. 2. Approximately, nearly NIR-to-NIR UC emission can be achieved in $KY_{2.97}Nd_{0.03}F_{10}$ phosphors under the single NIR (808 nm) wavelength excitation pumped by a conventional LD.
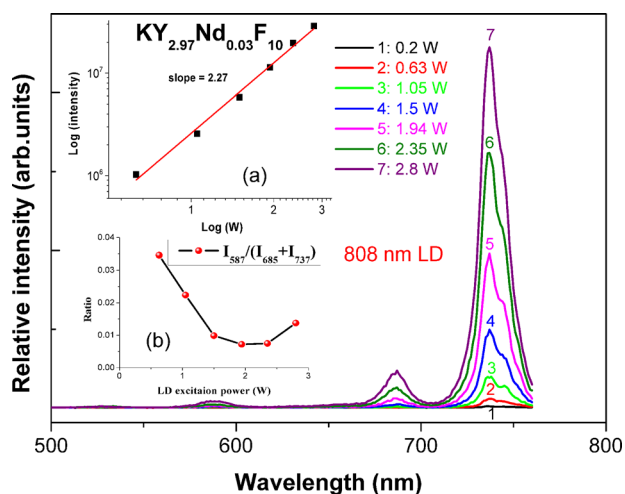

FIG. 2. The UC emission spectra of $KY_{2.97}Nd_{0.03}F_{10}$ upon 808 nm laser excitation with different power. The inset (a) shows the log–log plots of emission intensity versus 808 nm laser excitation power. The inset (b) shows the ratio of $I_{587}/(I_{685} + I_{737})$ versus 808 nm laser excitation power.
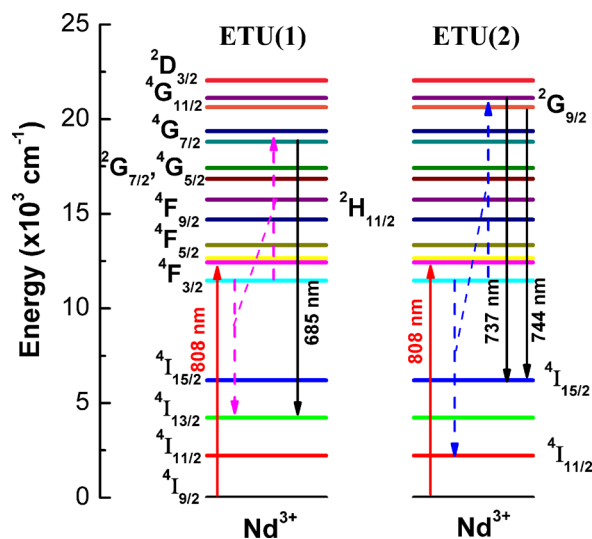

FIG. 3. Energy level diagram for Nd^{3+} doped KY_3F_{10} and possible upconversion mechanism related to ETU.

In general, visible emission lines assigned to transitions from the $^4G_{7/2}$ and $^4G_{5/2}$ levels are routinely seen in the UC emission spectra of many Nd-doped PL materials.[25–27] The excited $^4G_{7/2}$ level could be populated based on two possible mechanisms, namely, excited state absorption (ESA) and energy transfer upconversion (ETU). For ESA by an excitation at 808 nm, a previous population of the Nd^{3+} ions in the $^4F_{3/2}$ level is needed; the excited ions absorb photons reaching the excited $^2D_{5/2}$ level, from which they can decay to the $^4G_{7/2}$ level by non-radiative relaxation. In the case of ETU, pairs of Nd^{3+} ions are promoted to $^4F_{3/2}$ level interact: one ion of every pair decays non-radiatively to the $^4I_{13/2}$ state, transferring its energy to the other one, which reaches the $^4G_{7/2}$ level from which radiative emissions are possible, shown as ETU (1) in Fig. 3.

According to the energy levels of Nd^{3+} in the sample $KY_{2.97}Nd_{0.03}F_{10}$, the most likely cross relaxation energy transfer process is to populate the NIR emitting levels after the absorption of one NIR photon, i.e., $^4F_{3/2} + {}^4F_{3/2} \rightarrow {}^4I_{11/2} + {}^2G_{9/2}$. In this process, when two Nd^{3+} ions are excited to the $^4F_{3/2}$ state, a transfer process occurs by which one ion loses energy and goes to the $^4I_{11/2}$ state, while the other one gains energy and goes to the $^2G_{9/2}$ state, described in the energy level diagram presented in Fig. 3 [ETU (2)]. According to our experimental results, we deduce that the UC mechanism in the $KY_{2.97}Nd_{0.03}F_{10}$ sample is mainly based on ETU (2). Since the host KY_3F_{10} owns low phonon energy with $\sim$400 cm^{-1}, the phonon relaxation at the $^2G_{9/2}$ level could be effectively reduced. The influence of phonon assisted relaxation of the $^2G_{9/2}$ level state becomes small by F level states; therefore, radiative emission from the $^2G_{9/2}$ level state can be generated. It is interesting to note the fact that both the excitation and emission wavelengths fall into the "biological optical windows" (NIR I) in the UC process of the sample KY_3F_{10} singly doped with ions, which is most desirable for a bioprobe.

Fig. 4(a) shows the NIR excitation and the emission spectra of the sample $KY_{2.97}Nd_{0.03}F_{10}$. Under 1055 nm NIR light monitoring, the excitation spectrum shows several sharp lines peaked at about 354, 469, 527, 584, 690, 746, and 801 nm, ascribed to $^4I_{9/2}$ to $^4D_{1/2}(^4D_{3/2})$, $^4G_{9/2}$, $^2K_{13/2}(^4G_{7/2})$,

$^4G_{5/2}(^2G_{7/2})$, $^4F_{9/2}$, $^4S_{3/2}(^4F_{7/2})$, and $^4F_{5/2}(^2H_{9/2})$ transitions, respectively. In addition, an incomplete broad band peaked at $\sim$218 nm can be observed in the excitation spectrum, which is probably attributed to the charge transfer state between O^{2-} and Nd^{3+} (Nd^{3+}-CTS) instead of the intrinsic band-to-band absorption edge of the host material.[28] From the excitation spectrum, one can draw a conclusion that there are strong absorptions near 800 nm wavelength in the single Nd^{3+} activated KY_3F_{10} phosphors. In the NIR stokes emission spectrum, it can be observed that three peaks are located at 890, 1055, and 1350 nm, which are ascribed to the electron transition in Nd^{3+} ions from the excited state $^4F_{3/2}$ to the ground state ^4I_J ($J = 9/2$, 11/2, and 13/2) upon 808 nm NIR light (Xe lamp). Among these emission intensities, the transition from $^4F_{3/2}$ to $^4I_{11/2}$ ($\sim$1055 nm) is overwhelmingly dominant.

Fig. 4(b) shows the decay curve for the $KY_{2.97}Nd_{0.03}F_{10}$ sample emission at 1055 nm under the excitation at 808 nm. The curve is well fitted by the bi-exponential equation[29]

$$I_t = I_0 + A_1 \exp(-t/\tau_1) + A_2 \exp(-t/\tau_2), \qquad (1)$$

where I is the luminescence intensity, A_1 and A_2 are constants, t is the time, and τ_1 and τ_2 are the decay times for the bi-exponential components, respectively. Furthermore, the lifetime of the nonexponential decay curve is determined by the expression of $\tau_{ave} = \frac{A_1\tau_1^2 + A_2\tau_2^2}{A_1\tau_1 + A_2\tau_2}$. The values of τ_1, τ_2, and τ_{ave} are calculated from the fitted curves, as shown in Fig. 4(b). The decays of $^4F_{3/2}$ are non-monoexponential, due to the energy transfer mechanism by the cross relaxation among Nd^{3+} energy levels, which occurs readily at a relatively high concentration with 1 mol%. According to the energy level of Nd^{3+}, as displayed in Fig. 3, a possible cross-relaxation process is as follows: $^4F_{3/2} + {}^4F_{3/2} \rightarrow {}^4I_{11/2} + {}^2G_{9/2}$ and $^4F_{3/2} + {}^4F_{3/2} \rightarrow {}^4I_{13/2} + {}^4G_{7/2}$.

In addition to the above UC PL, NIR DS emission spectra of $KY_{2.97}Nd_{0.03}F_{10}$ were obtained under the same pumping source of 808 nm LD. As shown in Fig. 5, a similar emission profile was apparent in the sample when pumping with different incident power. The dominant emission peak
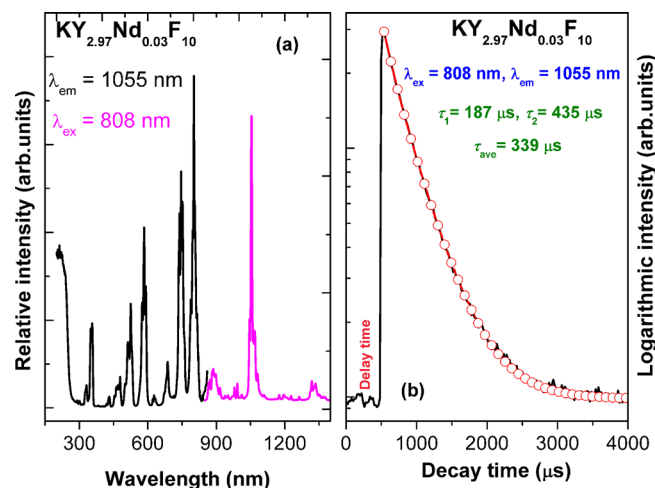

FIG. 4. (a) The excitation ($\lambda_{em} = 1055$ nm) and emission ($\lambda_{ex} = 808$ nm) spectra of $KY_{2.97}Nd_{0.03}F_{10}$. (b) The decay curves of $KY_{2.97}Nd_{0.03}F_{10}$ upon 808 nm excitation with 1055 nm emission wavelength.
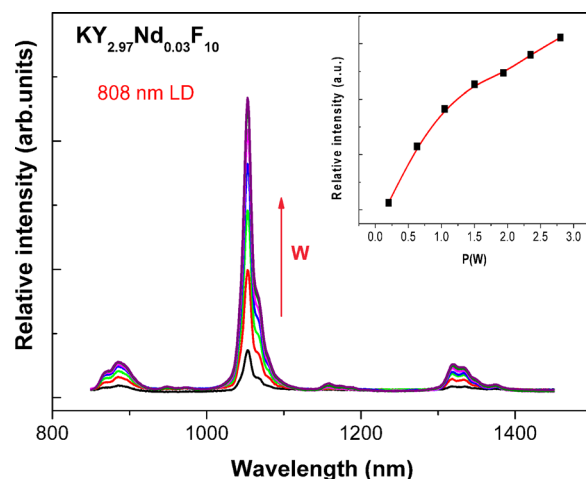

FIG. 5. The DS emission spectra of the sample $KY_{2.97}Nd_{0.03}F_{10}$ upon 808 nm laser excitation with different excited power. The inset shows the emission intensities vs 808 nm laser power.

is also located at 1055 nm. Moreover, it is found that the emission intensity of Nd^{3+} increases when increasing the excited power. The inset of Fig. 5 shows the emission intensities versus the incident power. DS luminescence involves the conversion from a high energy photon to low energy one. In contrast to the UC process, DS possesses much higher quantum yield. Similar to the above UC process, both the excitation (NIR I) and emission (NIR II) lie within the dual "biological optical windows" in the observed DS process as displayed in Fig. 5. Two channels of UC and DS are simultaneously realized in a single compound pumped by 808 nm LD. In fact, the two modes are greatly beneficial for the bioimaging. The emission at the NIR I region produces higher signal-to-noise ratio images compared with the visible region because of the decreased background radiation.[30] On the other hand, the emission at the NIR II region offers an increased penetrating depth up to 4 cm,[31] by which the skull or brain of a small animal may be diagnosed by using the NIR luminescence of the Nd-doped probe.

Here, it is worth noting that UC and DS pumped by 808 nm LD are two competing processes with the $^4F_{3/2}$ state as a watershed. Hence, the domination of the primary process can be designed by controlling the population of the $^4F_{3/2}$ state with the experimental conditions such as doping ion concentration, temperature, and laser power. Obviously, in the KY_3F_{10} host, the Nd^{3+} concentration plays a key role. The mechanism of NIR I-to-NIR I UC is related to ETU by $^4F_{3/2} + {}^4F_{3/2} \rightarrow {}^4I_{11/2} + {}^2G_{9/2}$ cross relaxation in KY_3F_{10}:1 mol% Nd^{3+} phosphors, leading to strong NIR UC emission. When decreasing the doping Nd^{3+} concentration (e.g., 0.01% mol), the probability of the above mentioned cross relaxation will hardly occur. Then, the dominant process is NIR I-to-NIR II DS and vice versa.

In conclusion, the UC and DS spectral properties of the sample KY_3F_{10} singly doped with 1 mol% Nd^{3+} ions have been systematically investigated. Dual-mode functions of NIR I-to NIR to-NIR I UC or NIR I-to-NIR II DS have been realized under 808 nm LD excitation, which exhibit NIR UC emissions dominated at 737 nm and NIR DS emissions dominated at 1055 nm. The KY_3F_{10}:Nd^{3+} nanocrystals are expected to be used in *in vitro* and *in vivo* bioimaging applications. It should be noted that the form of nanocrystals or colloidal solution prepared by different methods would be crucial to the future bioimaging application. In this connection, the optical properties and luminescence efficiencies would have some changes relevant to the material's factors such as particle morphology and size distribution.

[1]M. F. Tsai, S. H. G. Chang, F. Y. Cheng, V. Shanmugam, Y. S. Cheng, C. H. Su, and C. S. Yeh, ACS Nano **7**(6), 5330 (2013).

[2]Y. M. Yang, Q. Zhao, W. Feng, and F. Y. Li, Chem. Rev. **113**, 192 (2013).

[3]W. Zheng, P. Huang, D. T. Tu, E. Ma, H. M. Zhu, and X. Y. Chen, Chem. Soc. Rev. **44**, 1379 (2015).

[4]J. Zhou, Z. Liu, and F. Y. Li, Chem. Soc. Rev. **41**, 1323 (2012).

[5]M. K. Tsang, G. X. Bai, and J. H. Hao, Chem. Soc. Rev. **44**, 1585 (2015).

[6]A. M. Smith, M. C. Mancini, and S. M. Nie, Nat. Nanotechnol. **4**, 710 (2009).

[7]F. Wang and X. G. Liu, J. Am. Chem. Soc. **130**, 5642 (2008).

[8]Q. Liu, W. Feng, and F. Y. Li, Coord. Chem. Rev. **273–274**, 100 (2014).

[9]L. Z. Zhao, J. J. Peng, Q. Huang, C. Y. Li, M. Chen, Y. Sun, Q. N. Lin, L. Y. Zhu, and F. Y. Li, Adv. Funct. Mater. **24**, 363 (2014).

[10]C. X. Li, Z. H. Xu, D. M. Yang, Z. Y. Cheng, Z. Y. Hou, P. Ma, H. Z. Lian, and J. Lin, CrystEngComm **14**, 670 (2012).

[11]H. T. Wong, H. L. W. Chan, and J. H. Hao, Opt. Express **18**, 6123 (2010).

[12]D. Wang, B. Xue, X. G. Kong, L. P. Tu, X. M. Liu, Y. L. Zhang, Y. L. Chang, Y. S. Luo, H. Y. Zhao, and H. Zhang, Nanoscale **7**, 190 (2015).

[13]D. Jaque and J. García Solé, Phys. Rev. B **70**, 155116 (2004).

[14]T. Kushida, H. M. Marcos, and J. E. Geusic, Phys. Rev. **167**, 289 (1968).

[15]Y. F. Wang, G. Y. Liu, L. D. Sun, J. W. Xiao, J. C. Zhou, and C. H. Yan, ACS Nano **7**, 7200 (2013).

[16]Z. P. Wu, G. X. Bai, Q. R. Hu, D. Y. Guo, C. L. Sun, L. Y. Ji, M. Lei, L. H. Li, P. G. Li, J. H. Hao, and W. H. Tang, Appl. Phys. Lett. **106**, 171910 (2015).

[17]R. J. R. Vieira, L. Gomes, J. R. Martinelli, and N. U. Wetter, Opt. Express **20**, 12487 (2012).

[18]E. van der Kolk, P. Dorenbos, K. Krämer, D. Biner, and H. U. Güdel, Phys. Rev. B **77**, 125110 (2008).

[19]B. Ahrens, C. Eisenschmidt, J. A. Johnson, P. T. Miclea, and S. Schweizer, Appl. Phys. Lett. **92**, 061905 (2008).

[20]B. Ahrens, P. T. Miclea, and S. Schweizer, J. Phys.: Condens. Matter **21**, 125501 (2009).

[21]H. M. da Silva, M. D. Linhares, A. F. H. Librantz, L. Gomes, L. C. Courrol, S. L. Baldochi, and I. M. Ranieri, J. Appl. Phys. **109**, 083533 (2011).

[22]A. Rapaport, J. Milliez, F. Szipocs, M. Bass, A. Cassanho, and H. Jenssen, Appl. Opt. **43**, 6477 (2004).

[23]K. Friese, H. Krüger, V. Kahlenberg, T. Balić-Zunić, H. Emerich, J. Y. Gesland, and A. Grzechnik, J. Phys.: Condens. Matter **18**, 2677 (2006).

[24]M. Suáreza, A. Fernández, J. L. Menéndez, M. Nygren, Z. Zhao, R. Torrecillas, A. M. Pabloc, P. Haro-Gonzálezc, J. J. Romerod, and I. R. Martínc, Ceram. Int. **40**, 15951 (2014).

[25]Cz. Koepke, K. Wisniewski, L. Sikorski, D. Piatkowski, K. Kowalska, and M. Naftaly, Opt. Mater. **28**, 129 (2006).

[26]O. S. Wenger, D. R. Gamelin, H. U. Güdel, A. V. Butashin, and A. A. Kaminskii, Phys. Rev. B **61**, 16530 (2000).

[27]R. Balda, J. Fernandez, M. A. Arriandiaga, and J. M. Fernandez-Navarro, J. Phys.: Condens. Matter **19**, 086223 (2007).

[28]S. Kamimura, C. N. Xu, H. Yamada, N. Terasaki, and M. Fujihala, Jpn. J. Appl. Phys., Part 1 **53**, 092403 (2014).

[29]S. L. Dong, H. H. Lin, T. Yu, and Q. Y. Zhang, J. Appl. Phys. **116**, 023517 (2014).

[30]X. J. Niu, H. Y. Chen, Y. Q. Wang, W. H. Wang, X. Y. Sun, and L. X. Chen, ACS Appl. Mater. Interfaces **6**, 5152 (2014).

[31]R. Weissleder, Nat. Biotechnol. **19**, 316 (2001).